

Synthesis and Characterization of Amphiphilic Hydroxypropylcellulose-graft-Poly(ϵ -caprolactone)

Ruiwen Shi, Helen M. Burt

Faculty of Pharmaceutical Sciences, University of British Columbia, 2146 East Mall, Vancouver, British Columbia, Canada V6T 1Z3

Received 1 July 2002; accepted 20 October 2002

ABSTRACT: An amphiphilic graft copolymer, hydroxypropylcellulose-graft-poly(ϵ -caprolactone) (HPC-g-PCL), was synthesized by bulk polymerization without a catalyst and characterized with one-dimensional and two-dimensional NMR spectroscopy. Molar substitution of ϵ -caprolactone on HPC (MS_{CL}) was estimated by both gravimetry and 1H -NMR, and the gravimetric method was considered suitable for MS_{CL} determination. Heterogeneity in the HPC-g-PCL film was suggested by a microscopic study, and the exis-

tence of PCL-rich crystalline regions was confirmed by the results of X-ray diffraction and differential scanning calorimetry (DSC). The double endotherm observed in the DSC scans of HPC-g-PCL was associated with the different molecular weight fractions in the copolymer. © 2003 Wiley Periodicals, Inc. *J Appl Polym Sci* 89: 718–727, 2003

Key words: synthesis; graft copolymers; polysaccharides; NMR; amphiphiles

INTRODUCTION

Amphiphilic copolymers have been widely used as emulsifiers, dispersants, and surface stabilizers.^{1–3} Micelles formed from amphiphilic block copolymers have been recognized as an important type of pharmaceutical vehicle because of their ability to solubilize hydrophobic drugs.⁴ Because poly(ethylene glycol) (PEG) is biocompatible and highly water soluble, block copolymers with PEG as the hydrophilic component have been the most extensively investigated amphiphilic copolymers.⁴ A variety of polymers have been used to build the hydrophobic blocks. These include polymers of ϵ -caprolactone (CL),^{5,6} lactide,^{7,8} glycolide,⁸ aspartic acid,⁹ β -benzyl aspartate,¹⁰ and propylene oxide.¹¹ These copolymers have been widely investigated as biodegradable carriers for the controlled release of drugs and as amphiphilic micellizing agents for the solubilization of hydrophobic drugs.

During the past few years, increased interest has been shown in amphiphilic graft copolymers of hydrophilic polysaccharides. Water-soluble polysaccharides, such as starch,¹² dextran,¹³ and pullulan,^{14,15} have been used as main-chain polymers with hydrophobic poly(ϵ -caprolactone) (PCL), polylactide, and polyglycolide as side chains. Graft copolymerizations have been initiated by the hydroxyl groups of the

polysaccharides and catalyzed by stannous 2-ethylhexanoate. The enzyme-catalyzed graft copolymerization of CL onto hydroxyethylcellulose films was also reported recently.¹⁶

In our laboratory, we are developing film formulations based on biodegradable, biocompatible polysaccharides for the controlled delivery of hydrophobic drugs such as paclitaxel. However, paclitaxel precipitates out within the matrix of water-soluble polysaccharides because of its hydrophobicity.¹⁷ Hydroxypropylcellulose (HPC) is widely used as a pharmaceutical excipient for various purposes, including as a binding agent in tablet or granule formulations, a film-coating material, and a thickening agent.¹⁸ It is water soluble when it contains at least 2 mol of combined propylene oxide per anhydroglucose unit. The synthesis of a graft copolymer of HPC with hydrophobic PCL side chains should increase the hydrophobicity of the resulting copolymer and potentially make it a more suitable carrier for hydrophobic drugs.

In this study, a biodegradable HPC-g-PCL graft copolymer was synthesized by ring-opening polymerization without a catalyst. To our knowledge, this is the first literature report of both the synthesis without a catalyst and the characterization of HPC-g-PCL.

EXPERIMENTAL

Materials

HPC with a nominal molecular weight of 100,000 was purchased from Aldrich (Milwaukee, WI) and was dried at room temperature under reduced pressure (0.3 mmHg) for 16 h. CL was purchased from Fluka

Correspondence to: H. M. Burt (burt@interchange.ubc.ca).
Contract grant sponsor: Angiotech Pharmaceuticals, Inc.

(Milwaukee, WI). It was dried over calcium hydride (Fluka, Buchs, Switzerland) for 24 h and distilled twice under reduced pressure. Tetrahydrofuran (THF; high performance liquid chromatography (HPLC) grade), hexanes (certified American Chemical Society), methanol (HPLC grade), and acetonitrile (HPLC grade) were purchased from Fisher Scientific (Fairlawn, NJ), and deuterated dimethyl sulfoxide (DMSO- d_6 ; D = 99.9%) and deuterated chloroform ($CDCl_3$; D = 99.8%) from Cambridge Isotope Laboratories, Inc. (Andover, MA), were used as received.

Synthesis of HPC-g-PCL

HPC-g-PCL graft copolymer was synthesized by a bulk polymerization method. HPC and CL were added into a dry flask at a ratio of 1:4 (wt/wt), mixed thoroughly, and left at room temperature overnight until HPC was fully swelled by CL. The mixture was placed under a vacuum (0.3 mmHg) for 30 min and purged with nitrogen gas. The purging process was repeated three times. The flask was then sealed under a nitrogen blanket and placed in an oil bath at 150°C for 24 h.

Determination of the conversion of CL

The unreacted CL was extracted from the original reaction product and assayed by HPLC as follows: The reaction product was accurately weighed and dissolved in THF. An excess amount of hexanes was added to the solution to precipitate the polymers. The supernatant was collected, dried under nitrogen gas, reconstituted with distilled water, and injected into a Waters HPLC instrument (Milford, MA). The instrument was equipped with a model 600 controller and pump module, a model 486 ultraviolet detector, a model 717+ autosampler, and Millennium³² software for instrument control and data analysis. The column was an Aqua C18 (Phenomenex, Torrance, CA), and the mobile phase was methanol/water (35/65) at a flow rate of 0.5 mL/min.

Purification and fractionation of HPC-g-PCL

PCL homopolymer formed during the reaction and unreacted CL were removed by fractional precipitation with THF as the solvent and hexanes as the precipitant. The reaction product was dissolved in THF at a concentration of 5% (w/v). Hexanes with a volume equal to that of the solution were added under agitation to precipitate HPC-g-PCL. The mixture was left at room temperature for 30 min to allow for complete precipitation. The dissolution and precipitation were repeated three times.

A solution of HPC-g-PCL, purified with the method described previously, was prepared in THF with a

concentration of 3% (w/v). Hexanes were added to the solution to precipitate higher molecular weight fractions [hexanes molar fraction (X_H) = 0.327]. The system was allowed to stand at room temperature until the two phases could be physically separated (~30 min was required). The supernatant was collected and dried to give the first fraction (F1). The precipitate was dissolved in THF, and hexanes with a lower molar fraction were added. The procedures were repeated to yield three more fractions (F2, F3, and F4). The F4 fraction was the precipitate in the last cycle. All of the fractions were dried at room temperature. The X_H values used for the fractionation of HPC-g-PCL are given in Table III (shown later).

Gel permeation chromatography (GPC)

HPC-g-PCL purity and its molecular weight and molecular-weight distribution were determined with a Waters GPC system, which was equipped with the same components as the HPLC instrument except that a model 2410 refractive index detector was used in this study. HR3 and HR4 Styragel columns (Milford, MA) were used in series. The mobile phase was THF at a flow rate of 1.0 mL/min. Polystyrene standards were used to construct a calibration curve that was used to calculate the molecular weight and molecular-weight distribution.

NMR

¹H-NMR, ¹³C-NMR spectra, and two-dimensional heteronuclear multiple quantum coherence (HMQC) spectra of HPC and HPC-g-PCL were recorded with a Bruker (Rheinstetten, Germany) AMX500 spectrometer operating at 95°C. Two-dimensional correlation spectroscopy studies were performed with a 90°- t_1 -45°- t_2 pulse sequence (COSY-45) with a Bruker AV400 spectrometer operating at 95°C. Samples were dissolved in DMSO- d_6 . ¹H-NMR spectra of PCL homopolymer and the fractions of HPC-g-PCL were acquired with a Bruker WH400 spectrometer operating at 25°C. The samples were dissolved in $CDCl_3$.

Morphology of the HPC-g-PCL films

HPC-g-PCL films were prepared by a solution casting method. A solution of HPC-g-PCL in THF with a concentration of 30 mg/mL of was cast into Teflon dishes and dried at room temperature (ca. 20°C) in the fume hood for 48 h. The films were further dried at room temperature under reduced pressure for another 48 h.

Optical microscopy studies of HPC-g-PCL films were conducted with an Olympus BH-2 optical microscope, and photographs were taken at a magnification of 150× with a Contax 167MT camera.

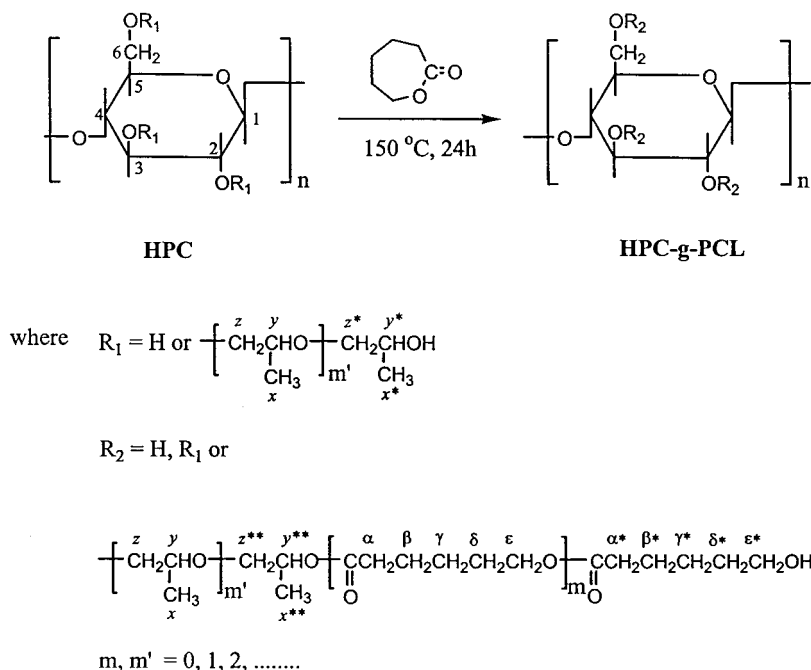


Figure 1 Chemical structures of HPC and HPC-g-PCL and the reaction scheme. x, y, z , and all Greek symbols represent a specific position in the molecule. For example, H_x and H_{x^*} denote methyl protons in given positions in the chain, as shown.

A Rigaku (Tokyo, Japan) Rotaflex X-ray diffractometer equipped with a rotating target X-ray tube and a wide-angle goniometer was used to obtain the diffraction patterns of HPC-g-PCL films. The X-ray source was $K\alpha$ radiation from a copper target with a graphite monochromator. The X-ray tube was operated at a potential of 50 kV and a current of 150 mA. The range (2θ) of scans was from $10\text{--}30^\circ$, and the scan speed was $2^\circ/\text{min}$ at increments of 0.02° .

Differential scanning calorimetry (DSC) was conducted with a PerkinElmer (Norwalk, CT) Pyris 1 instrument. Fresh HPC-g-PCL films were weighed (3–5 mg) into nonhermetic aluminum pans and subjected to a heating/cooling/reheating cycle from -100 to 100°C at $10^\circ\text{C}/\text{min}$ with liquid nitrogen as a coolant and helium as a purge gas. The films were also annealed at 37°C for a week and then heated at $10^\circ\text{C}/\text{min}$ in the same temperature range.

RESULTS AND DISCUSSION

Synthesis and purification of HPC-g-PCL

The ring-opening polymerization of CL to form either a homopolymer or copolymers has been investigated extensively. In most of the studies, the polymerization was initiated by a system consisting of compounds containing hydroxyl groups, such as alcohols, and Lewis acids, such as stannous 2-ethylhexanoate, and various mechanisms were proposed. In some studies, it was suggested that the Lewis acids acted as catalysts and that the acids were not covalently bonded to the

polymer chains.^{19–23} In other studies,^{24–26} Lewis acids were considered to be co-initiators that were covalently bonded to the polymer chains. However, some studies have clearly shown that hydroxyl-group-containing compounds alone can initiate CL polymerization. Without Lewis acids, polymerizations are restricted to the synthesis of low-molecular-weight polymers.^{19,27}

As shown in Figure 1, HPC is a hydroxyl-group-rich polymer. On each repeat unit, there are three hydroxyl groups. In this work, the graft copolymerization of CL

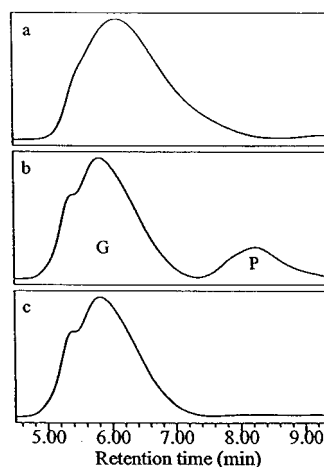


Figure 2 GPC chromatograms of (a) backbone HPC and (b) the reaction product, in which G represents the HPC-g-PCL component and P represents the PCL homopolymer formed during the reaction, and (c) purified HPC-g-PCL.

TABLE I
Results for the Synthesis of Four Batches of HPC-g-PCL with a Feed Ratio of 1:4 of the Starting Materials HPC and CL

Batch No	Reaction scale (g) ^a	HPC-g-PCL ^b		PCL ^c		CL conversion (%) ^f	Yield (%) ^g	MS _{CL} ^h
		$M_w \times 10^{-5}$ ^d	M_w/M_n ^e	$M_w \times 10^{-3}$ ^d	M_w/M_n ^e			
1	5	3.17	1.7	3.10	1.2	71.0	62.8	10.1
2	5	3.18	1.7	3.08	1.2	71.6	62.8	10.1
3	5	3.10	1.8	2.97	1.2	72.5	62.9	10.1
4	150	2.99	1.8	2.68	1.2	61.8	56.7	8.6

M_n = number-average molecular weight.

^a The sum of the feed amounts of HPC and CL.

^b Graft copolymer formed during the reaction corresponding to component G in Figure 2(b).

^c PCL homopolymer formed during the reaction corresponding to component P in Figure 2(b).

^d Measured by GPC and calculated by Millennium³² software based on the polystyrene standard curve. The mobile phase was THF at 1 mL/min. The columns used were Styragel HR3 and HR4 in series.

^e Polydispersity index, determined with the same method used for determining M_w .

^f Calculated from the amount of reacted CL divided by the feed amount of CL.

^g Calculated from the weight of the purified HPC-g-PCL divided by the total weight of the reactants.

^h Determined with the gravimetric method.

was initiated by these hydroxyl groups. Because we intended for the PCL side chains to be short, a catalyst was not used. GPC chromatograms of the starting material HPC and the reaction product are shown in Figure 2(a,b). Before grafting, HPC had one peak at a retention time of 6.1 min. After grafting, the peak shifted to a lower retention time region (the component represented by peak G) and became bimodal. The shift indicated an increase in molecular weight, indicative of graft copolymer formation. Peak G became bimodal because the peak for the HPC starting material [Fig. 2(a)] had a shoulder at a retention time of around 5.2–5.4 min, and this shoulder was amplified after the graft reaction. The chromatogram also showed another peak between 7.5 and 9.5 min (the component represented by the broad peak P). This peak was due to PCL homopolymer formed during the graft reaction. The component represented by peak P could no longer be detected after the purification process, as shown in Figure 2(c). The results of the synthesis of four batches of HPC-g-PCL are summarized in Table I. The four batches were synthesized at the same feed ratio of HPC and CL (1:4) but with different scales. In batches 1, 2, and 3, 1 g of HPC and 4 g of CL were added into the flasks, and the syntheses were carried out under the same conditions. The reproducibility of the reaction was demonstrated by the small variance among the three batches in the conversions of CL, the yields, the molecular weights, the polydispersity indices of HPC-g-PCL, and the molar substitution of ϵ -caprolactone on HPC (MS_{CL}). In batch 4, the synthesis was carried out on a much larger scale (30-fold) under the same conditions. As expected, both conversion and yield decreased, and the resulting HPC-g-PCL had a lower molecular weight and MS_{CL}. The weight-average molecular weight (M_w) of the start-

ing material HPC determined by GPC was 2.01×10^{-5} . After the grafting reaction, the M_w of HPC-g-PCL was 3×10^{-5} , indicating the formation of the graft copolymer. The M_w of the PCL homopolymer formed during the reaction was close to 3000.

Evidence of graft copolymer formation from NMR spectroscopy

¹H-NMR spectroscopy is one of the most powerful tools for both qualitative and quantitative analysis of polymer structure. HMQC spectroscopy was used to correlate the ¹³C-NMR spectra with ¹H-NMR spectra and to obtain information on C—H connectivity. COSY was used to correlate the coupled nuclei so that the changes in chemical shifts caused by the graft copolymerization could be identified. In this work, COSY-45 was used to record the crosspeaks that occurred between the directly connected transitions.

The ¹H-NMR spectrum of component P (data not shown) was identical to those previously reported and could be readily assigned.^{28,29} The ϵ protons had peaks at two different chemical shifts, 3.56 and 3.99 ppm. The peak at 3.56 ppm was assigned to the ϵ protons in the repeating units at the PCL chain ends.²⁸ The assignments are given in Table II. The ¹H-NMR spectra of HPC and component G are shown in Figures 3 and 4, respectively. The spectra were recorded in DMSO-d₆ at 95°C to improve the resolution.³⁰ In the spectrum of HPC (Fig. 3), a peak at a chemical shift of 4.4 ppm was observed. In the HMQC spectra (data not shown), a crosspeak clearly indicated the connectivity between C1 at 101.1 ppm and the proton at 4.4 ppm. Therefore, the peak at 4.4 ppm was assigned to the anomeric proton at C1. The peak at 1.06 ppm was assigned to the methyl protons in the hydroxypropyl groups (H_X).^{30,31} The ¹H-NMR spectrum of component

TABLE II
Observed Chemical Shifts (δ s) in the ^1H -NMR Spectra of Purified HPC-g-PCL and PCL Homopolymer Formed During the Reaction

HPC-g-PCL (component G) ^a				PCL (component P) ^b	
^{13}C	δ (ppm)	^1H	δ (ppm)	^1H	δ (ppm)
C_x	16.56	H_x	1.06	—	—
C_x^*	19.42	H_x^*	1.06	—	—
C_x^{**}	15.99	H_x^{**}	1.16	—	—
$\text{C}_y(\text{C}_y^*)$	64.97	$\text{H}_y(\text{H}_y^*)$	3.5–3.7	—	—
C_y^{**}	68.56	H_y^{**}	4.90	—	—
C_α	32.97	H_α	2.27	H_α	2.23
C_β	23.52	H_β	1.5–1.6	H_β	1.5–1.6
C_γ	24.41	H_γ	1.35	H_γ	1.31
C_δ	27.31	H_δ	1.5–1.6	H_δ	1.5–1.6
C_δ^*	31.55	H_δ^*	1.44	H_δ^*	—
C_ϵ	62.91	H_ϵ	4.01	H_ϵ	3.99
C_ϵ^*	60.18	H_ϵ^*	3.42	H_ϵ^*	3.56
$\text{C}=\text{O}$	171.95				

C or H atoms labeled with a subscript denote C or H atoms in a given position in the molecule, as shown in Fig. 1.

^a Spectrum recorded at 500 MHz and 95°C with DMSO- d_6 as the solvent.

^b Spectrum recorded at 400 MHz and 25°C with CDCl_3 as the solvent.

G (shown in Fig. 4) contained peaks from both HPC and PCL, indicating HPC-g-PCL formation. On the basis of the spectra assignments of HPC and PCL, the major peaks in Figure 4 were assigned. The COSY-45 spectrum of component G, shown in Figure 5, provided more information about the interactions between protons within HPC-g-PCL and enabled the assignment of the small peaks in the ^1H -NMR spectrum (Fig. 4). The peak assignments are given in Table II. The labeling of the protons and carbons is shown in Figure 1.

The methyl peak at 1.06 ppm in the ^1H -NMR spectrum of HPC (Fig. 3) split into two in that of

HPC-g-PCL, with one remaining at the chemical shift of 1.06 ppm and another shifting to a lower field (1.16 ppm; Fig. 4). The shifted peak corresponded to the methyl protons in the hydroxypropyl groups connecting directly to the PCL chains ($\text{H}_{x^{**}}$). The shift was due to the deshielding effect of ester groups formed during the graft reaction. In addition, there was another small broad peak at 4.9 ppm in the ^1H -NMR spectrum of HPC-g-PCL. Neither HPC nor PCL had this peak in their spectra. Crosspeak 1 in the COSY-45 spectrum (Fig. 5) indicated that the protons corresponding to this peak (at 4.9 ppm) coupled with the methyl protons with a

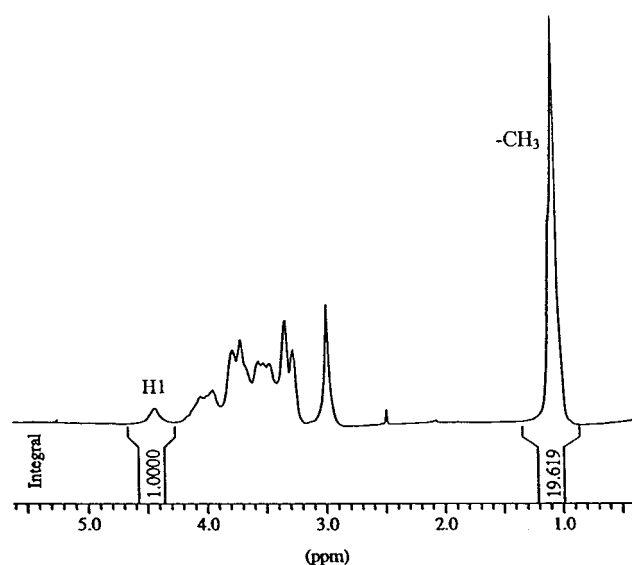


Figure 3 ^1H -NMR spectrum of HPC in DMSO- d_6 recorded at 95°C with a Bruker AMX500 spectrometer.

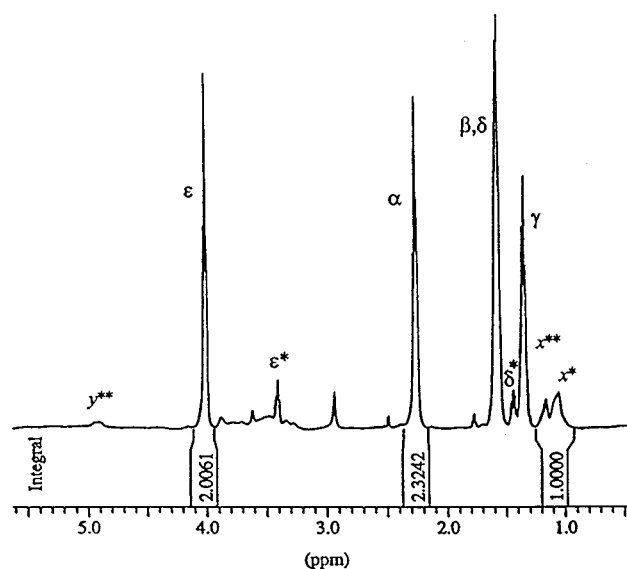


Figure 4 ^1H -NMR spectrum of HPC-g-PCL in DMSO- d_6 recorded at 95°C with a Bruker AMX500 spectrometer.

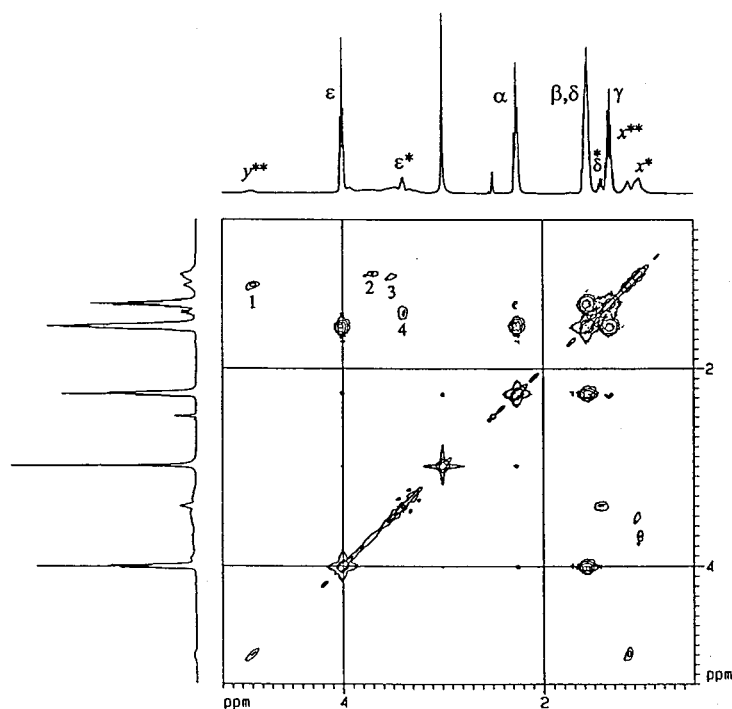


Figure 5 COSY-45 spectrum of HPC-g-PCL in DMSO- d_6 recorded at 95°C with a Bruker AMX500 spectrometer.

chemical shift of 1.16 ppm. Therefore, these were methine protons in the hydroxypropyl groups connecting directly to the PCL chains ($H_{y^{**}}$). The methine protons in the hydroxypropyl substituents (H_y and H_{y^*} (see Fig. 1 for the definition of H_x , H_{x^*} , $H_{y'}$ and H_{y^*})) that did not react with CL were located in the range 3.5–3.7 ppm. This was supported by cross-peaks 2 and 3, which revealed the H_{x^*} – H_{y^*} and H_x – H_y (see Fig. 1 for the definition of H_x , H_{x^*} , $H_{y'}$ and H_{y^*}) coupling, respectively. The shift from 3.5 to 4.9 ppm is a typical change for an acylation reaction.³² This was considered to be additional evidence for the formation of the graft copolymer.

Crosspeak 4 in the COSY spectrum in Figure 5 indicated that the protons at the chemical shift of 1.44 ppm coupled with ϵ protons in the repeating units at the PCL chain ends (ϵ^* protons). Therefore, the small peak at 1.44 ppm was assigned to δ protons in the repeating units at the PCL chain ends (δ^*).

Molar substitution (MS)

The way in which substituents are bonded to a polysaccharide molecule may be described in terms of MS, which is the average number of substituent molecules that have reacted with each anhydroglucose unit.³¹ In HPC-g-PCL molecules, there were two different substituents on the cellulose chains: hydroxypropyl groups and PCL chains. To calculate MS_{CL} , it was necessary to first determine the molar substitution of

the hydroxypropyl groups on the cellulose chains (MS_{HP}).

MS_{HP} was estimated with the 1H -NMR spectroscopy method.^{30,31} The method is based on the fact that each different proton in different structural groups gives rise to peaks at a characteristic magnetic field strength, and the peak intensity is directly proportional to the concentration of the protons. Peak intensity in an 1H -NMR spectrum is affected by experimental parameters such as pulse angle and relaxation delay. 1H -NMR spectra for both HPC and HPC-g-PCL were acquired with a pulse angle of 36° and a relaxation delay of 2 s. To ensure reliable peak intensities, spectra were also acquired at relaxation delays of 4 and 8 s, respectively. The spectra obtained with the three different relaxation delays gave identical peak intensities, indicating that the peak intensities used in the following calculations were quantitatively reliable.

As shown in the structure of HPC in Figure 1, each hydroxypropyl group brings to the cellulose skeleton three methyl protons, and each anhydroglucose unit has one anomeric proton connecting to C1. Therefore, MS_{HP} can be determined with the peak intensities of these two types of protons in the HPC spectrum:

$$MS_{HP} = (I_{CH_3}/3)/I_{H1}$$

where I_{CH_3} is the peak intensity of the methyl group and I_{H1} is the peak intensity of the anomeric proton at C1. MS_{HP} was calculated as 6.5, which means on av-

erage, there were 6.5 hydroxypropyl groups connected to each anhydroglucose unit. On the basis of this value, the average formula weight of the repeating unit of HPC was calculated as 539.

MS_{CL} was estimated in a similar way with the relative intensities of the peaks for PCL and HPC in the 1H -NMR spectrum of purified HPC-g-PCL, and a MS_{CL} value (22.7) higher than the initial feed molar ratio was obtained, indicating that the spectroscopy method was not suitable. A similar result was reported for dextran-g-PCL.¹³ The errors were considered to be primarily from peak integration, especially when the PCL content in the graft copolymer was high. As shown in Figure 4, the peaks from the backbone HPC were broad and small compared to those from the side-chain PCL. This could have brought about significant errors in the peak integration, which subsequently affected the results of MS_{CL} .

MS_{CL} was then determined with a gravimetric method. The calculation is given as follows:

$$MS_{CL} = [(W_{\text{graft}} - W_{\text{HPC}}) / 114] / (W_{\text{HPC}} / 539)$$

where W_{graft} is the weight of HPC-g-PCL after purification, W_{HPC} is the initial weight of HPC, 114 is the formula weight of a repeating unit of PCL, and 539 is the average formula weight of a repeating unit of HPC. In this calculation, HPC was assumed to be 100% converted to HPC-g-PCL. The results for the four different batches are given in Table I.

Side-chain length and distribution

On the basis of the assignment and integration of the 1H -NMR spectrum of HPC-g-PCL, the average length of the PCL side chains (\bar{L}) and the number of the side

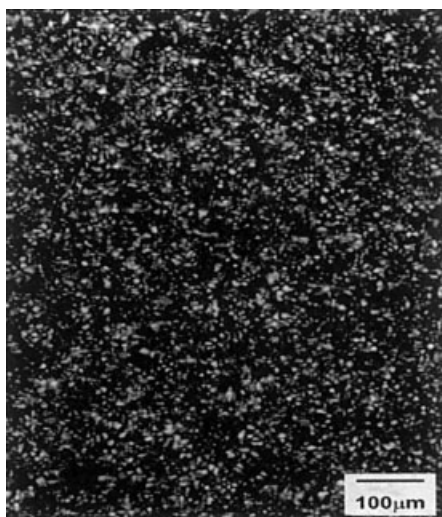


Figure 6 Optical microscopy of HPC-g-PCL film under polarizing lens.

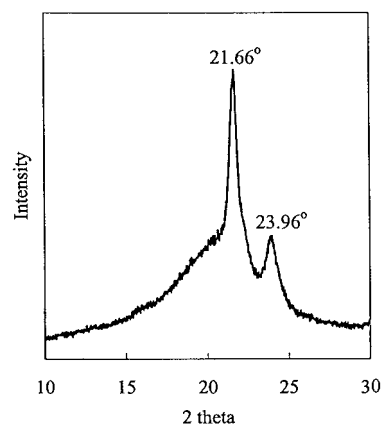


Figure 7 Representative X-ray diffraction pattern of the HPC-g-PCL film cast from THF solution.

chains on each HPC repeating unit could be estimated. \bar{L} can be calculated from the peak intensity of ϵ^* protons and the total peak intensities of all of the ϵ protons in PCL chains. However, an accurate peak intensity for the ϵ^* protons cannot be obtained because of peak overlap. Theoretically, the number of ϵ protons is equal to that of α protons. Therefore, the peak intensity for α protons ($I_{H\alpha}$) is used as an equivalent of the total intensity for all of the ϵ protons, and the calculation is given by

$$\bar{L} = I_{H\alpha} / (I_{H\alpha} - I_{H\epsilon})$$

where $I_{H\epsilon}$ is the peak intensity of the ϵ protons that are not at the chain end and $I_{H\alpha}$ is the peak intensity of the α and α^* protons (peaks overlapped). The \bar{L} of HPC-g-PCL synthesized in batch 4 was 7.3. The average number of PCL chains on each HPC repeating unit (\bar{N}) was then calculated by

$$\bar{N} = MS_{CL} / \bar{L}$$

On the basis of the MS_{CL} determined with the gravimetric method, \bar{N} for HPC-g-PCL in batch 4 was 1.2. Hence, on average, there were 12 PCL side chains attached to 10 HPC repeating units.

Morphological study of HPC-g-PCL

A two-phase morphology is commonly observed for graft copolymers with components that differ remarkably in their properties.³³ In HPC-g-PCL, the HPC backbone was water soluble, whereas the PCL side chain was hydrophobic. HPC-g-PCL film cast from THF solution was examined with an optical microscope with a polarizing lens. The regular pattern, shown in Figure 6, suggested heterogeneity in the film. Because PCL is a semicrystalline polymer, we speculated that the microcrystalline regions repre-

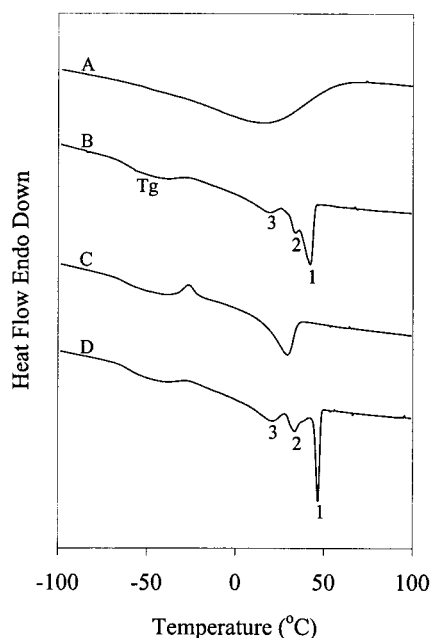


Figure 8 Representative DSC scans of HPC-g-PCL films cast from THF solution: (A) the first heating scan of the freshly prepared films, (B) the second heating scan of the freshly prepared films, and (C) the first heating scan of the films annealed at 37°C for a week.

sented by the bright spots were likely due to the formation of a PLC-rich phase, and there was a possibility that the HPC backbone component may have coexisted in the PCL-rich phase.

An X-ray diffraction pattern of the HPC-g-PCL film is shown in Figure 7. Diffraction peaks were located at diffraction angles (2θ) of 21.66 and 23.96°, in agreement with those reported for PCL in the literature.³⁴ These results suggest that the partially crystalline phase in the film of HPC-g-PCL originated from the PCL side chains.

DSC analysis provided further evidence for the existence of a partially crystalline PCL phase in the HPC-g-PCL film. DSC scans of HPC-g-PCL films sub-

jected to different temperature programs are shown in Figure 8. The heating scan of the fresh HPC-g-PCL films (curve B) showed one glass-transition temperature (T_g) and three endotherms. T_g occurred at -72°C (onset), in agreement with the T_g for the PCL homopolymer. The main endotherm (peak 1) appeared at 41.8°C (peak temperature) with a shoulder (peak 2) at 32.7°C and was attributed to the melting of the PCL crystalline phase. The nature of the small endotherm at 20°C (peak 3) was uncertain. A broad peak occurred at the same temperature in the scan of HPC [Fig. 8(A)], which indicated that peak 3 might have originated from the HPC backbone. The second heating scan [Fig. 8(C)] showed a T_g at the same position as that in Figure 8(B), a recrystallization peak at -27°C , and a broad endotherm with a peak at 28.7°C . This decrease in the melting temperature (T_m) revealed that a less ordered crystalline structure was formed during the relatively fast cooling/reheating cycle ($10^\circ\text{C}/\text{min}$), compared to the much slower solidification of the films in the solution casting process that took approximately 24 h. Figure 8(D) is a heating scan for the HPC-g-PCL films annealed at 37°C for a week, in which peak 1 moved to a higher temperature (46.2°C) and peak 2 remained at the same position. The increase in the temperature of peak 1 indicated that a more ordered crystalline structure formed during the annealing. The nature of peaks 1 and 2, and the reason that the peak 2 position did not change could be explained by the following studies on the fractions of HPC-g-PCL.

Characterization of the fractions of HPC-g-PCL

Purified HPC-g-PCL was fractionated, and the fractions were characterized by GPC, DSC, and $^1\text{H-NMR}$. The X_H values in the precipitating solvent, the molecular weights, and molecular-weight distributions are given in Table III.

$^1\text{H-NMR}$ spectra of the fractions were obtained at 25°C , and all four fractions had identical $^1\text{H-NMR}$

TABLE III
Physicochemical Data on HPC-g-PCL (F0) and Its Four Fractions (F1, F2, F3, and F4) Produced by Precipitation from the THF Solution with Different X_H

Fraction	X_H^a	M_w (kg mol^{-1}) ^b	M_w/M_n^b	T_g ($^\circ\text{C}$) ^c	T_m ($^\circ\text{C}$) ^d	ΔH_f (J/g) ^e
F0	—	368	1.52	-72.3 ± 1.8	47.1 ± 2.4	28.3 ± 2.1
F1	0.327	133	1.33	-71.6 ± 0.7	46.2 ± 1.5	36.5 ± 1.8
F2	0.275	184	1.34	-72.4 ± 1.5	44.1 ± 1.3	30.4 ± 1.7
F3	0.249	330	1.30	-72.8 ± 0.5	42.0 ± 0.9	19.8 ± 1.1
F4	0.240	554	1.10	-72.7 ± 0.6	41.5 ± 0.9	11.2 ± 1.7

The values in columns 5 to 7 represent mean plus or minus standard deviation ($n = 3$).

^a Molar fractions of hexanes in the precipitating solvent.

^b Measured by GPC in THF, with polystyrene standards.

^c Onset values of the glass transitions.

^d Endpoint of the melting endotherm.

^e Heat of fusion of the double melting endotherm

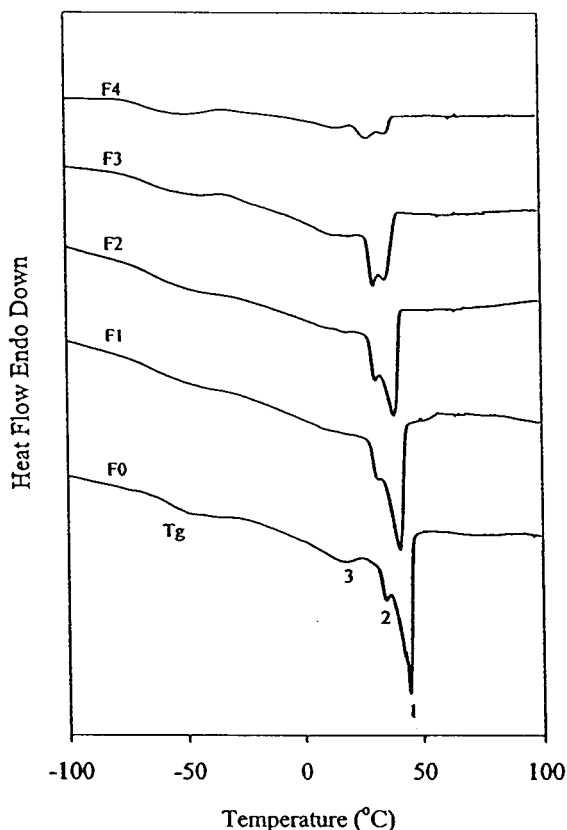


Figure 9 Representative DSC scans of HPC-g-PCL (F0) and the four fractions (F1, F2, F3, and F4). The samples were films cast from THF solutions. The heating rate was 10°C/min.

spectra, indicating that the four fractions were the graft copolymer HPC-g-PCL. Hence, the assumption that 100% of HPC was converted to HPC-g-PCL was appropriate.

DSC scans of the four fractions are shown in Figure 9. The thermal transition temperatures (T_g and T_m) and heat of fusion (ΔH_f) data are given in Table III. The T_g 's for the four fractions were similar, at approximately -72°C , and all four DSC scans possessed a double-melting endotherm in the temperature range 20 – 50°C . However, the relative sizes of peaks 1 and 2 in the double-melting endotherm were quite different. In the scan for F1, peak 1 constituted the major part of the melting endotherm. The relative size of peak 2 increased with the increasing molecular weight of the fractions. In the scan for F4, the size of peak 2 exceeded that of peak 1 and became a major component of the melting endotherm. These results suggest that the two peaks in the HPC-g-PCL double-melting endotherm originated from different fractions in the copolymer. The high-molecular-weight fractions had lower melting ranges and were largely responsible for the lower temperature part of the melting endotherm. The low-molecular-weight fractions had higher melting ranges and were mainly responsible for the higher

temperature part of the melting endotherm. This was an unexpected finding given the normal relationship between T_m and molecular weight and may have been a result of the sample preparation method. In this work, the samples for the DSC measurements were prepared by the solution casting method. In the concentrated solutions of the copolymer, the polymer chains of the high-molecular-weight fractions were less mobile than those of the low-molecular-weight fractions, thus crystallites were formed with a lower degree of perfection. Consequently, the high-molecular-weight fractions had lower T_m 's than the low-molecular-weight fractions. The significant difference in ΔH_f for different fractions (Table III) may have been a function of crystallinity and/or the degree of perfection of the crystallites.

CONCLUSIONS

The amphiphilic graft copolymer HPC-g-PCL was synthesized by bulk polymerization without a catalyst. The evidence for the graft reaction was obtained with both one-dimensional and two-dimensional NMR spectroscopy. The downfield shift of the ^1H -NMR peaks corresponding to H_y and H_x was considered to be direct evidence for the graft polymerization. MS_{CL} was determined to be in the range 8.6 – 10.1 by a gravimetric method, and the average PCL side-chain length was estimated to be 7.3 by NMR spectroscopy. The films cast from the solution of the copolymer were heterogeneous due to the formation of PCL-rich microcrystalline regions. DSC and X-ray diffraction data indicated that the partially crystalline phase was PCL. The double-melting endotherm observed in the DSC originated from different molecular weight fractions of HPC-g-PCL. The low melting endotherm was associated with the high-molecular-weight fractions, and the high melting endotherm was associated with the low-molecular-weight fractions.

The authors thank Colin Fyfe, Ziwei Xiao, and Lu Yang for their help with the NMR experiments.

References

- Xie, H.-Q.; Wu, X.-D.; Guo, J.-S. *J Appl Polym Sci* 1994, 54, 1079.
- Garti, N. *Acta Polym* 1998, 49, 606.
- Martinez, G.; Sanchez-Chaves, M. *Revista Plast Modernos* 2001, 81, 482.
- Torchilin, V. P. *J Controlled Release* 2001, 73, 137.
- Yuan, M.; Wang, Y.; Li, X.; Xiong, C.; Deng, X. *Macromolecules* 2000, 33, 1613.
- Allen, C.; Han, J.; Yu, Y.; Maysinger, D.; Eisenberg, A. *J Controlled Release* 2000, 63, 275.
- Zhang, X.; Jackson, J. K.; Burt, H. M. *Int J Pharm* 1996, 132, 195.
- Li, Y.; Kissel, T. *J Controlled Release* 1993, 27, 247.
- Kataoka, K.; Kwon, G. S.; Yokoyama, M.; Okana, T.; Sakurai, Y. *J Controlled Release* 1993, 24, 119.

10. Kwon, G. S.; Naito, M.; Yokoyama, M.; Okano, T.; Sakurai, Y.; Kataoka, K. *Langmuir* 1993, 9, 945.
11. Miller, D. W.; Batrakova, E. V.; Waltner, T. O.; Alakhov, V. Y.; Kabanov, A. V. *Bioconjugate Chem* 1997, 8, 649.
12. Choi, E.-J.; Kim, C.-H.; Park, J.-K. *Macromolecules* 1999, 32, 7402.
13. Ydens, I.; Rutot, D.; Degee, P.; Six, J.-L.; Dellacherie, E.; Dubois, P. *Macromolecules* 2000, 33, 6713.
14. Donabedian, D. H.; McCarthy, S. P. *Macromolecules* 1998, 31, 1032.
15. Ohya, Y.; Maruhashi, S.; Ouchi, T. *Macromolecules* 1998, 31, 4662.
16. Li, J.; Xie, W.; Cheng, H. N.; Nickol, R. G.; Wang, P. G. *Macromolecules* 1999, 32, 2789.
17. Jackson, J.; Skinner, K. C.; Burgess, L.; Sun, T.; Hunter, W. L.; Burt, H. M. *Pharm Res* 2002, 19, 411.
18. Kibbe, A. H. *Handbook of Pharmaceutical Excipients*, 3rd ed.; American Pharmaceutical Association: Washington, DC, 2000.
19. Schindler, A.; Hibionada, Y. M.; Pitt, C. G. *J Polym Sci Polym Chem Ed* 1982, 20, 319.
20. Du, Y. J.; Lemstra, P. J.; Nijenhuis, A. J.; Aert, H. A. M. V.; Bastiaansen, C. *Macromolecules* 1995, 28, 2124.
21. Schwach, G.; Coudane, H.; Engel, R.; Vert, M. *J Polym Sci Part A: Polym Chem* 1997, 35, 3431.
22. Kricheldorf, H. R.; Kreiser-Saunders, I.; Boettcher, C. *Polymer* 1995, 36, 1253.
23. Veld, P. J. A. I. T.; Velnor, E. M.; Witte, P. V. D.; Hamhuis, J.; Dijkstra, P. J. *J Polym Sci Part A: Polym Chem* 1997, 35, 219.
24. Ryner, M.; Stridsberg, K.; Albertsson, A.-C. *Macromolecules* 2001, 34, 3877.
25. Kowalski, A.; Duda, A.; Penczek, S. *Macromolecules* 2000, 33, 689.
26. Kowalski, A.; Duda, A.; Penczek, S. *Macromolecules* 2000, 33, 7359.
27. Brode, G. L.; Koleske, J. V. *J Macromol Sci Chem* 1972, 6, 1109.
28. Jacquier, V.; Miola, C.; Llauro, M.-F.; Monnet, C.; Hamaide, T. *Macromol Chem Phys* 1996, 197, 1311.
29. Kricheldorf, H. R.; Kreiser, I. *J Macromol Sci Chem* 1987, 24, 1345.
30. Robitaille, L.; Turcotte, N.; Fortin, S.; Charlet, G. *Macromolecules* 1991, 24, 2413.
31. Ho, F. F.-L.; Kohler, R. R.; Ward, G. A. *Anal Chem* 1972, 44, 178.
32. Simons, W. W.; Zanger, M. *The Sadtler Guide to NMR Spectra*; Sadtler Research Laboratories: Philadelphia, 1972.
33. Noshay, A.; McGrath, J. E. *Block Copolymers: Overview and Critical Survey*; Academic: New York, 1977.
34. Ong, C. J.; Price, F. P. *J Polym Sci Polym Symp* 1978, 63, 45.